Nix alone is sufficient to convert female *Aedes aegypti* into fertile males and *myo-sex* is needed for male flight

Azadeh Aryan[a,b], Michelle A. E. Anderson[a,b,1], James K. Biedler[a,b], Yumin Qi[a,b], Justin M. Overcash[c], Anastasia N. Naumenko[b,d], Maria V. Sharakhova[b,d,e], Chunhong Mao[f], Zach N. Adelman[c], and Zhijian Tu[a,b,2]

[a]Department of Biochemistry, Virginia Tech, Blacksburg, VA 24061; [b]Fralin Life Science Institute, Virginia Tech, Blacksburg, VA 24061; [c]Department of Entomology, Texas A&M University, College Station, TX 77843; [d]Department of Entomology, Virginia Tech, Blacksburg, VA 24061; [e]Laboratory of Ecology, Genetics, and Environment Protection, Tomsk State University, 634041 Tomsk, Russia; and [f]Biocomplexity Institute & Initiative, University of Virginia, Charlottesville, VA 22911

A dominant male-determining locus (M-locus) establishes the male sex (M/m) in the yellow fever mosquito, *Aedes aegypti*. *Nix*, a gene in the M-locus, was shown to be a male-determining factor (M factor) as somatic knockout of *Nix* led to feminized males (M/m) while transient expression of *Nix* resulted in partially masculinized females (m/m), with male reproductive organs but retained female antennae. It was not clear whether any of the other 29 genes in the 1.3-Mb M-locus are also needed for complete sex-conversion. Here, we report the generation of multiple transgenic lines that express *Nix* under the control of its own promoter. Genetic and molecular analyses of these lines provided insights unattainable from previous transient experiments. We show that the *Nix* transgene alone, in the absence of the M-locus, was sufficient to convert females into males with all male-specific sexually dimorphic features and male-like gene expression. The converted m/m males are flightless, unable to perform the nuptial flight required for mating. However, they were able to father sex-converted progeny when presented with cold-anesthetized wild-type females. We show that *myo-sex*, a myosin heavy-chain gene also in the M-locus, was required for male flight as knockout of *myo-sex* rendered wild-type males flightless. We also show that *Nix*-mediated female-to-male conversion was 100% penetrant and stable over many generations. Therefore, *Nix* has great potential for developing mosquito control strategies to reduce vector populations by female-to-male sex conversion, or to aid in a sterile insect technique that requires releasing only non-biting males.

mosquito | sex-determination | M factor | infectious diseases | *Aedes aegypti*

Highly diverse primary signals serve as the master switches to initiate sex-determination in insects (reviewed in ref. 1). In some species the initiating signals are female-determining factors that trigger female development. For example, a double dose of the X-linked signal elements in the fruit fly *Drosophila melanogaster* instigates female development in XX embryos (2); in honey bees the heterozygosity of the *complementary sex determiner* (*csd*) gene initiates female development in diploid embryos produced by fertilized queen bees (3); and a W chromosome-linked Piwi-interacting RNA gene determines female sex in ZW silkworms (4). In contrast, a dominant male-determining factor (M factor) serves as the primary signal that triggers male development in many other insects, including mosquitoes and other non-*Drosophila* flies, beetles, and true bugs (1, 5–8). The M factor is located either on a Y chromosome or within a sex locus named the M-locus on a homomorphic sex-determining chromosome, both of which are repeat-rich and thus difficult to study. Facilitated by recent advances in bioinformatics and genetic technologies, the M factor has been discovered in five dipteran insects, including *Nix* in the yellow fever and dengue fever mosquito *Aedes aegypti* (9), *gYG2/Yob* in the African malaria mosquito *Anopheles gambiae* (10, 11), *Guy1* in the Asian malaria mosquito *Anopheles stephensi* (12), *Mdmd* in the housefly *Musca domestica*

(13), and *MoY* in the Medfly *Ceratitis capitata* (14). None of these M factors are apparently related to each other, indicating frequent turnover of the initiating signals for sex-determination. However, through a cascade of events, these highly divergent primary signals are eventually transduced as sex-specific isoforms of conserved transcription factors doublesex (DSX) and fruitless (FRU) that program sexual differentiation. Thus, diverse primary signals in different species regulate the alternative, sex-specific splicing of *dsx* and *fru* pre-mRNAs, leading to sex-specific DSX and FRU protein isoforms.

Sex conversion resulting from a loss-of-function mutant male or a gain-of-function female would strongly indicate that an M factor is the master switch for sex determination. Such evidence has been presented only in species for which sex chromosome dosage compensation is not necessary or where the M factor may not be involved in dosage compensation (9, 13). We have previously shown that somatic knockout of *Nix* in male embryos resulted in feminized *Ae. aegypti* adults with developing ovaries, and female embryos injected with a plasmid that contains the *Nix* ORF driven by a strong constitutive promoter (polyUb) developed into partially masculinized adults (9). However, full phenotypic sex

---

Significance

The presence of a dominant male-determining locus (M-locus) in one of a pair of autosomes establishes the male sex in the dengue fever mosquito *Aedes aegypti*. The *Ae. aegypti* M-locus contains 30 genes, including *Nix*, a previously reported male-determining factor. Here we show that the *Nix* transgene alone was sufficient to convert females into fertile males, which continued to produce sex-converted progeny. We also show that a second M-locus gene named *myo-sex* was needed for male flight. *Nix*-mediated sex conversion was 100% penetrant, heritable, and stable, indicating great potential for developing mosquito-control strategies to reduce vector populations by female-to-male conversion. This work also sheds lights into the molecular basis of the function of the M-locus.

---

conversion was not observed, presumably due to somatic mosaicism, the transient nature of *Nix* expression, or the use of a different promoter. Moreover, the *Ae. aegypti* M-locus contains four other protein-coding and 25 long-noncoding RNA (lncRNA) genes, several of which showed highly enriched expression in the testes and male accessory glands (15). Thus, it remains unclear whether *Nix* alone is sufficient for conferring complete male sexually dimorphic traits and fertility.

Here, we present molecular and genetic characterizations of *Nix*-transgenic lines and show that the *Nix* transgene alone, in the absence of the M-locus, is sufficient to convert females into fertile males with all male-specific sexually dimorphic features. We show that a second M-locus gene named *myo-sex* is needed for male flight. We also show that *Nix*-mediated sex conversion is 100% penetrant, heritable, and highly stable, indicating great potential for developing mosquito control strategies to reduce vector populations by female-to-male sex conversion. This work will also inform future investigations into homomorphic sex chromosomes that are found in other insects, vertebrates, and plants.

Results

Generation of *Nix* Transgenic Lines. Initial efforts failed to produce transgenic lines when *Nix* was under the control of the polyUb promoter. Thus, we sought to make transgenic mosquitoes that stably express a *Nix* transgene under the control of its native promoter. We isolated a 2.5-kb region upstream of the *Nix* gene, which was used to express the *Nix* transgene in the plasmid (Fig. 1*A*). In addition to the native *Nix* ORF (N1), we also designed a second plasmid that contains a Strep II tag (16) at the N terminus (N2) to facilitate future biochemical studies and to distinguish between the endogenous *Nix* and the *Nix* transgene (Fig. 1*A*). Three transgenic lines were obtained (*SI Appendix,* Tables S1–S3) using the plasmids shown in Fig. 1*A*. In subsequent analyses we focused on two of these (one line derived from each of the two constructs), hereto referred to as N1 and N2. The transgene insertion sites were identified by inverse PCR (*SI Appendix,* Fig. S1; primers are shown in *SI Appendix,* Table S4). Bioinformatic mapping of the sequences flanking the N2 transgene revealed an insertion on chromosome 2 (Fig. 1*B*), while the N1 transgene was present near the telomere on the 1p arm of chromosome 1 (Fig. 1*B*), distantly linked to the native M-locus, as confirmed by chromosomal fluorescence in situ hybridization (FISH) (Fig. 1*C*). To determine whether the native *Nix* promoter fragment recapitulated *Nix* expression in the context of these new genomic locations, we determined the transcription profile of the N2 transgene using primers that readily distinguish the N2 *Nix* transcript from the endogenous *Nix* transcript (*SI Appendix,* Fig. S2 and Table S4). Like the endogenous *Nix*, N2 *Nix* transcription was observed from the onset of embryonic development starting 2 to 4 h after egg deposition throughout all developmental stages. The N2 *Nix* transcript was detected in transgenic m/m pupae and adults but not in wild-type male pupae or adults. Also as expected, we did not observe endogenous *Nix* transcripts in transgenic m/m pupae or adults. Thus, the 2.5-kb *Nix* promoter that we isolated appears to function similarly to the native *Nix* promoter in the M-locus in its temporal expression pattern.

Transgenic *Nix* Causes Female-to-Male Sex Conversion. We next determined the phenotype of the genetic females (as indicated by the lack of the M-locus including *myo-sex* and the native *Nix* gene) (*SI Appendix,* Fig. S3) that contained the N1 or N2 *Nix* transgene. Four different genotypes are possible from crosses between transgenic males and wild-type females (Fig. 2*A*). They can be distinguished by the presence or absence of the EGFP transgenic marker (N/+ vs. $^{+/+}$) and the presence or absence of the endogenous M-locus (M/m vs. m/m) (*SI Appendix,* Fig. S3). All genetic females with the N2 transgene showed conversion to complete male sexually dimorphic features, including plumose antennae, external genitalia showing male gonocoxite and gonostylus, and internal sex organs such as testes and male accessory glands (Fig. 2 *B* and *C* and *SI Appendix,* Fig. S3). The same female-to-male conversion phenotype was also observed in the N1 line (*SI Appendix,* Fig. S4). Thus, the *Nix* transgene alone converted females into phenotypic males. The sex-converted males showed a slightly larger body size compared to the wild-type and
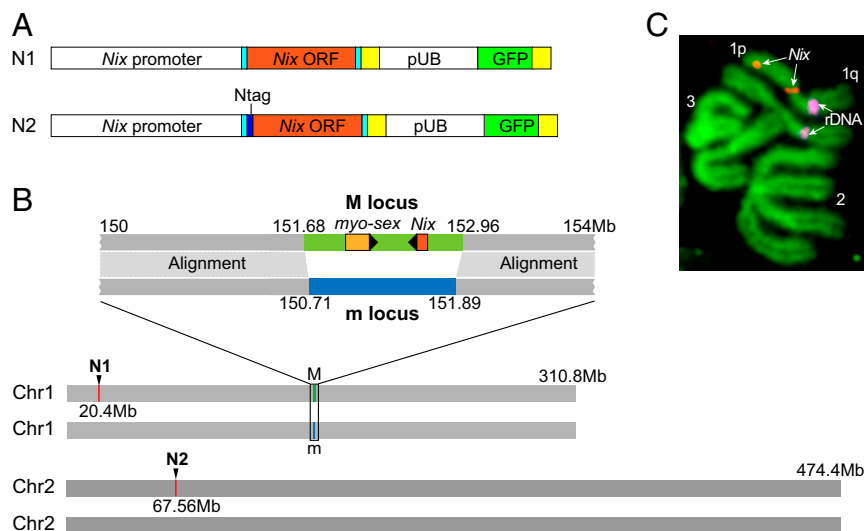
Fig. 1. Transgenic lines that stably express the *Nix* transgene. (*A*) Plasmid constructs used to create transgenic lines that stably express the *Nix* transgene. N1 was designed to express *Nix* from its own promoter. A 3.7-kb *Nix* sequence containing the ~2.5-kb promoter, the 5′UTR (light blue), the *Nix* ORF (orange), and 3′UTR (light blue) is followed by the SV40 polyadenylation signal (yellow). This *Nix* expression cassette is followed by the transformation marker cassette, GFP driven by the *Ae. aegypti* polyubiquitin promoter. These two cassettes are flanked by the Mos1 transposon arms, which are not shown (37). The N2 construct is identical to N1 except that a Strep-tag II (16) was added to the N terminus of the *Nix* ORF. (*B*) A schematic drawing showing the insertion sites in the N1 and N2 transgenic lines, respectively. The relative position of M and m loci and the content of known genes in the M-locus are also shown. (*C*) Chromosomal in situ hybridization using the N1 plasmid as a probe showed a signal (red) on the p arm of chromosome 1 in addition to a signal in the known M-locus (15). The rDNA signal (magenta) was used as a landmark for the q arm of chromosome 1. Image was taken using 1000× magnification.
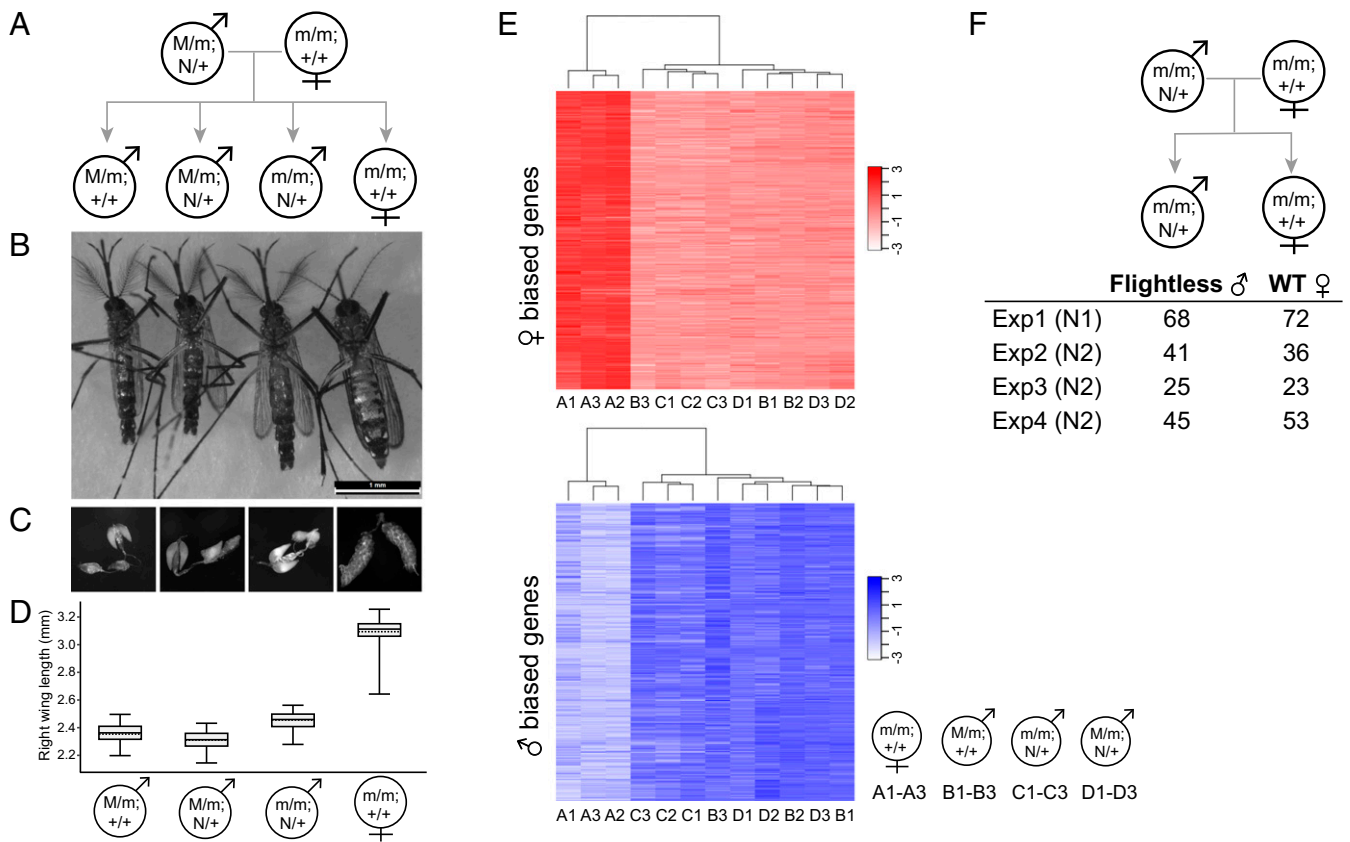
Fig. 2. The *Nix* transgene alone is sufficient to convert genetic females into fertile males with high penetrance and stability. (*A*) Pedigree showing the four genotypes of progeny from a cross between transgenic (N/+) males (M/m) and wild-type (+/+, or nontransgenic) females (m/m). N denotes the N1 or N2 *Nix* transgene. In this particular mating scheme, N2 transgenic males were used and produced progeny shown in *B–D*. (*B*) Representative individuals showing the phenotypes of the four genotypes shown in *A*. Genotyping was performed as shown in *SI Appendix*, Fig. S3. (*C*) Reproductive organs from individuals of the four genotypes. Images were taken using the LAS v4.5 software suite with 10× (whole body) or 40× (dissected tissues) magnification. (*D*) Length of the right wing of individuals of the four groups. Thirty individuals within each group were measured from the same cohort. Box plot, starting from bottom, shows minimum values, first quartile, median, third quartile, and maximum values using horizontal solid lines, with the mean indicated by a horizontal dashed line. As shown in *SI Appendix*, Table S5, all pairwise comparisons were significant ($P < 0.0001$), except for (M/m; $^{+/+}$) vs. (M/m; N2/+) males ($P = 0.1982$). (*E*) RNA-seq of biological triplicates of each of the four genotypes from a cross between N1 transgenic males and wild-type females. The log$_2$(FPKM+1) expression level heatmap of female-biased (red) and male-biased (blue) genes are shown and clustering of the samples was based on the transcription profile. (*F*) Mating of the sex-converted flightless m/m males with cold-anesthetized wild-type females produces wild-type females and m/m flightless males in four independent experiments. Similar results were obtained for both N1 and N2 (indicated in parentheses) transgenic m/m fathers. Genotype of the converted flightless males was confirmed (*SI Appendix*, Fig. S7).

transgenic M/m males, as indicated by their wing-length measurement (Fig. 2*D* and *SI Appendix*, Fig. S5 and Table S5), which is used as a reliable proxy for body size (17). It is possible that subtle differences in *Nix* transgene expression or other factors in the M-locus may contribute to the wing-length difference between sex-converted m/m males and M/m males. We performed RNA-sequencing (RNA-seq) analysis of three biological replicates of pooled individuals of the four genotypes (National Center for Biotechnology Information [NCBI] BioProject number PRJNA625258). The overall transcription profile of the sex-converted m/m males was highly similar to wild-type M/m and transgenic M/m males, but clearly different from the wild-type m/m females (Fig. 2*E* and *SI Appendix*, Tables S6–S8). In addition, *dsx* and *fru* splicing was shifted toward the male isoforms, as confirmed by digital-droplet RT-PCR (ddPCR) (*SI Appendix*, Fig. S6).

Males Converted from Females by *Nix* Are Flightless. Interestingly, all genetic females that were converted to phenotypic males due to the ectopic expression of the N1 or N2 transgene could not fly (Table 1; see also a video link at https://www.youtube.com/watch?v=fwUqN5iKTi0&feature=youtu.be). The majority of flightless

males were not able to completely fold their wings; they could walk and sometimes jump but could never sustain flight. Wild-type males, N1 or N2 M/m males, and wild-type females displayed normal flight phenotypes. To assess the stability of these phenotypes, we screened for the four genotypes over multiple generations by crossing either (M/m; N1/+) or (M/m; N2/+) males with wild-type females. Between the two lines, we found 0 transgenic individuals that developed as females, while scoring 4,541 transgenic males and 2,215 flightless transgenic males (Table 1). As

Table 1. Total number of progeny from crosses between transgenic males and wild-type females

Line	Transgenic ♂	Nontransgenic ♂	Transgenic ♀	Nontransgenic ♀	Transgenic flightless ♂
N1	2,696	829	0	2,186	902
N2	1,845	2,079	0	2,027	1,313

The latest screening was done for G$_{13}$ and G$_{15}$ for N1 and N2 lines, respectively. Detailed numbers from each generation are provided in *SI Appendix*, Tables S2 and S3.

expected, the percentage of flightless males were higher in the N2 line than the N1 line because N1 is linked to the M-locus while N2 is on a separate chromosome. However, the numbers of the four genotypes did not strictly follow the expected Mendelian segregation ratios in the N2 lines in some generations (*SI Appendix*, Table S3). It is possible that some N2 male converts may have died prior to adult emergence.

Males Converted from Females by *Nix* Are Fertile and the Sex-Conversion Phenotype Is Highly Penetrant and Heritable. We then tested whether N1 or N2 m/m males were fertile, despite the absence of the M-locus. As these converted males were flightless and flying is required during mating (18), they could not mate with females that are alert. However, in four independent experiments that include both N1 and N2 lines, the sex-converted males fathered viable progeny when placed with cold-anesthetized wild-type females in a confined space (Fig. 2F). As there is no M-locus at all in these sex-converted transgenic males (m/m; N/+), when mated with wild-type females (m/m; $^{+/+}$), only two genotypes are possible in their progeny: (m/m; N/+) and (m/m; $^{+/+}$), which will manifest as flightless sex-converted males and wild-type females, respectively. Indeed, flightless males and wild-type females were observed at an approximately 1:1 ratio in all four experiments, and genotyping results confirmed that these flightless males were indeed sex-converted genetic females (*SI Appendix*, Fig. S7). Thus, sex-converted phenotypic males are fertile and continued to produce sex-converted progeny, indicating that the *Nix* transgene alone is sufficient to convert females into fertile males and that this sex-conversion is heritable. These results, together with the fact that not a single transgenic individual developed a female phenotype over a combined 28 generations with thousands of individuals screened (Table 1), suggest that the female-to-male conversion conferred by the *Nix* transgene is highly penetrant and stable.

The Myosin Heavy-Chain Gene *Myo-Sex* Is Required for Male Flight. In addition to *Nix*, a myosin heavy-chain gene, *myo-sex* (19) is also located in the M-locus (15). *Myo-sex* and its closest autosomal paralog (AAEL005656) show sex-specific expression in males and females, respectively (19–21), and could be involved in sex-specific muscle functions. Therefore, we hypothesized that the flightless phenotype observed in N1 (m/m) and N2 (m/m) males is caused by the lack of the *myo-sex* gene associated with the M-locus. To test this hypothesis, we performed CRISPR/Cas9-mediated knockout using single-guide RNAs (sgRNAs) designed to specifically target the hemizygous *myo-sex* gene (Fig. 3). Following injection of preblastoderm embryos with a Cas9/sgRNA

mixture, a significant portion of the surviving G$_0$ males were flightless in three independent experiments. Despite the fact that only flying G$_0$ males produced progeny when wild-type females were provided for mating, a significant portion of the G$_1$ male offspring were also flightless in all three independent experiments (Fig. 3). We sequenced plasmids cloned from PCR products from 21 flightless G$_1$ males and identified mutations in the *myo-sex* gene in all of them. Thus, we conclude that the M-locus gene *myo-sex* is required specifically for male flight.

Transgenic and Nontransgenic Males Are Not Significantly Different in Reproductive Fitness under Laboratory Conditions. We performed competition assays by setting up six replicate cages, each containing 20 transgenic males (M/m; N/+) and 20 nontransgenic sibling males (M/m; $^{+/+}$) competing for 10 virgin Liverpool females. We recorded the number of transgenic and nontransgenic progeny of each female from all six cages for the N1 and N2 lines, respectively (*SI Appendix*, Table S9). Overall, the percent of females that produced broods that contained transgenic progeny was 51.9% and 55.8% for the N1 and N2 lines, respectively (*SI Appendix*, Table S10). However, this does not necessarily mean that the transgenic males are more competitive in mating than their nontransgenic siblings because we cannot assume that females mate only once (22). To investigate transgenic fitness, we focused on testing whether the proportion of transgenic progeny deviated from the expected 25% under the assumption of equal reproductive fitness between the hemizygous transgenic and nontransgenic males (Table 2). We note that this test does not assume that females mate only once or use sperm from just one male. Overall, the N1 cages produced 21.5% (603 of 2,802, 3.5% lower than expected) transgenic progeny, while the N2 cages produced 31.3% (721 of 2,303, 6.3% higher than expected) transgenic progeny. However, none of these differences were statistically significant.

Discussion

The generation and analyses of *Nix*-expressing transgenic lines (Fig. 1) provided insights unattainable from previous transient experiments. Here, we have shown that *Nix* alone fulfills the role of a dominant master switch for male determination in *Ae. aegypti*, converting females into fertile males (Fig. 2). The fact that *Nix* is transcribed at the onset of maternal-to-zygotic transition (9) and that *Nix* expression does not require any other factors in the M-locus, as shown by the transcription of the *Nix* transgene in m/m females (*SI Appendix*, Fig. S2), indicate that *Nix* is the primary signal in the sex-determination pathway.
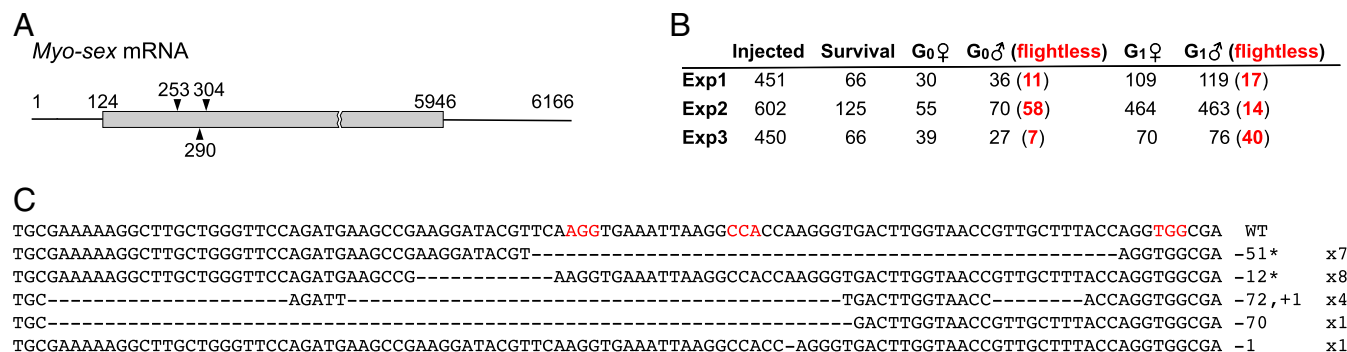

A

Myo-sex mRNA

B

	Injected	Survival	G$_0$♀	G$_0$♂ (flightless)	G$_1$♀	G$_1$♂ (flightless)
Exp1	451	66	30	36 (11)	109	119 (17)
Exp2	602	125	55	70 (58)	464	463 (14)
Exp3	450	66	39	27 (7)	70	76 (40)

C

```
TGCGAAAAAGGCTTGCTGGGTTCCAGATGAAGCCGAAGGATACGTTCAAGGTGAAATTAAGGCCACCAAGGGTGACTTGGTAACCGTTGCTTTACCAGGTGGCGA   WT
TGCGAAAAAGGCTTGCTGGGTTCCAGATGAAGCCGAAGGATACGT-------------------------------------------------AGGTGGCGA   -51*   x7
TGCGAAAAAGGCTTGCTGGGTTCCAGATGAAGCCG-----------AAGGTGAAATTAAGGCCACCAAGGGTGACTTGGTAACCGTTGCTTTACCAGGTGGCGA   -12*   x8
TGC-------------------AGATT------------------------------------------TGACTTGGTAACC-------ACCAGGTGGCGA   -72,+1   x4
TGC----------------------------------------------------------------------GACTTGGTAACCGTTGCTTTACCAGGTGGCGA   -70   x1
TGCGAAAAAGGCTTGCTGGGTTCCAGATGAAGCCGAAGGATACGTTCAAGGTGAAATTAAGGCCACC-AGGGTGACTTGGTAACCGTTGCTTTACCAGGTGGCGA   -1   x1
```

Fig. 3. *Myo-sex* knockout results in flightless males. (*A*) Three sgRNAs, starting at positions 253, 290, and 304, were used to target the *myo-sex* coding region, which spans positions 124 to 5,946. (*B*) CRISPR/Cas9-mediated *myo-sex* knockout produced flightless males in both the G$_0$ and G$_1$ generations in three independent experiments. G$_1$ progeny were produced only from crosses between wild-type virgin females and sgRNA+Cas9-injected flying G$_0$ males. (*C*) Sequence analysis of mutations in CRISPR/Cas9-edited flightless G$_1$ progeny. Top line denotes the wild-type sequence; subsequent lines show various mutant sequences. The number of deleted (−) and inserted (+) bases and their occurrence are indicated to the right; in-frame mutations are indicated by an asterisk; deleted bases are denoted by dashes. The PAM sites for the three sgRNAs are highlighted in red.

Table 2. Proportion of transgenic progeny

Replicate	+	−	Percent+, %
N1 replicate			
1	72	372	16.2
2	104	394	20.9
3	84	439	16.1
4	66	362	15.4
5	170	268	38.8
6	107	364	22.7
Total	603	2,199	21.5
N2 replicate			
1	57	279	17.0
2	129	378	25.4
3	154	329	31.9
4	148	214	40.9
5	108	118	47.8
6	125	264	32.1
Total	721	1,582	31.3

Generalized linear mixed-effect model analyses were performed to test the null hypothesis that 25% of the progeny will be transgenic under the assumption of equal reproductive fitness between the hemizygous transgenic and nontransgenic males. No statistically significant departure from the 25% expectation was detected for either N1 or N2 ($P > 0.05$). Power analysis by 1,000 simulations show that the probability to correctly reject the null hypothesis (at $\alpha = 0.05$) is 98.50% (95% confidence interval: 97.54 to 99.16%) and 99.10% (95% confidence interval: 98.30 to 99.59%) for N1 and N2, respectively. Data for each individual brood are provided in *SI Appendix*, Table S9. +, Number of transgenic (positive) progeny; −, number of nontransgenic (negative) progeny.

Therefore, we conclude that *Nix* is indeed the M factor for sex-determination in *Ae. aegypti*.

The *Ae. aegypti* M-locus is a 1.3-Mbp repeat-rich region that contains a total of 30 annotated genes (15). These include *Nix*, four other protein-coding genes, and 25 lncRNA genes, several of which showed highly enriched expression in the testes or male accessory glands (15). Although they are apparently not necessary for the sex conversion observed in this study, it is reasonable to speculate that some of these genes may be involved in male reproductive biology or male-specific behavior. We note that our mating assay is a test of the minimal requirement of male fertility. Therefore, our results should not be regarded as indication of a lack-of-function of other M-locus genes. In fact, the converted m/m males could not fly and thus mating with cold-anesthetized wild-type females was necessary. We show that knockout of *myo-sex*, another gene located in the M-locus, results in a flightless male phenotype and may explain why *Nix* alone cannot convert females to flying males. Although it remains unknown whether *Nix* and *myo-sex* together can transform genetic females into both fertile and flying males, this study defined the roles of two key protein-coding genes in the sex locus of a unique, homomorphic, sex-determining chromosome in an insect species having significant medical importance. This work will inform future investigations of homomorphic sex chromosomes that are found in other insects, vertebrates, and plants.

The high penetrance and stability of the *Nix* transgene make it an attractive candidate for manipulation to reduce the number of biting and egg-laying females. *Nix* transgenic males do not appear to be significantly different in reproductive fitness compared to their nontransgenic sibling males under laboratory conditions. To further assess the fitness-related parameters important for genetic applications, tests need to be performed with more replicates, larger sample sizes, and field-like conditions. Multiple transgenic lines and various populations should also be tested for position effect and population-specific parameters. Converting genetic females into flightless males by expressing an endogenous mosquito gene, *Nix*, already successfully removes

those females from the progeny. Although conceptually similar to female-killing approaches, the *Nix* transgenic males need not endure potentially leaky expression of a toxin designed to target females. To convert females into reproductively competitive males, a sex-conversion unit that includes both *Nix* and *myo-sex*, and possibly other M-locus genes, will be necessary. This may be achieved either by engineering a large sex-conversion cassette or by linking the necessary components in a region of suppressed recombination, which is not difficult to find in *Ae. aegypti* (15, 23, 24). Modeling suggests that the release of homozygous males carrying such a dominant sex-conversion unit is more effective than the sterile insect technique and the female-killing approaches in suppressing pest populations (25). The hemizygous *Nix* transgene in the current N1 and N2 males (M/m; N/+) is transmitted to only half of their progeny. The use of a conditional expression method, such as the tetracycline-repressible system (26), could allow for the development of homozygous strains carrying one or more copies of a *Nix* transgene or a sex-conversion unit. Such transgenic lines would produce male-only progeny and may be used as a population-suppression method (25, 27) or to significantly reduce the cost and augment the scale of other mosquito-control strategies that require the separation of males from females (28).

Nix-based female-removal or sex-conversion approaches could also be adapted to a homing-based gene-drive strategy (29) that would enable the inheritance of the transgene unit in almost all offspring, resulting in the removal or conversion of potentially all females. To mitigate resistance to homing, the *Nix*-containing homing cassette will need to target an essential gene (30–32). Here, sex-conversion is again much more powerful than female-removal. The outcome of releasing a sex-ratio distorter that is linked to a gene drive depends on the strength of the drive and the fitness of the transgenic individual (33, 34). Therefore, the successful design of a homing strategy for a sex-conversion unit requires balancing the need to transform females into sufficiently fit males using a multicomponent sex-conversion unit, and the ability to faithfully replicate that unit. Alternatively, the sex-conversion unit may be selected based on its linkage to a recoded essential gene that is no longer sensitive to a homing endonuclease that disrupts the endogenous copy of the essential gene (35).

Materials and Methods

Identification of the *Nix* Promoter Region. To isolate the promoter/upstream sequence of *Nix*, PCR was performed using two primers (*SI Appendix*, Table S4), one of which contained the *Nix* ORF and the other was from ~3 kb upstream. PCR was performed with an Arktik Thermal Cycler (Thermo Fisher Scientific) using *Ae. aegypti* (Liverpool) genomic DNA and the Q5 DNA Polymerase (New England Biolabs) according to the manufacturer's protocol, generating a single amplicon of ~3 kb. PCR products were cloned using the PCR-Blunt II-TOPO Cloning Kit (Thermo Fisher Scientific) and JM109 Competent Cells (Promega). A 2,575-bp sequence upstream of the ORF, a consensus derived from six clones, was used as the promoter. The ORF and the 5′ UTRs and 3′UTRs of *Nix* were previously determined (9).

Transgenic Constructs. As shown in Fig. 1*A*, the N1 construct was designed to express *Nix* from its own promoter. A 3.7-kb sequence containing the 2,575-bp promoter described above (including the 102-bp 5′ UTR), the 864-bp *Nix* ORF, and the 19-bp *Nix* 3′ UTR, followed by the SV40 polyadenylation/termination signal sequence was synthesized (Epoch Life Science), and cloned into the pM2_pUB_EGFP vector (36) using the PstI/AsiSI restriction sites. The pM2_pUB_EGFP vector consists of Mos1 transposase substrate arms and the EGFP transformation marker driven by the *Ae. aegypti* polyubiquitin promoter (36). The N2 construct was designed to allow NIX protein purification and identification via an N-terminal Strep-tag II (Trp-Ser-His-Pro-Gln_phe-Glu-Lys) (16), (Fig. 1*A*). The N2 construct is identical to N1 except that the Strep-tag II was added to the N terminus of the *Nix* ORF (synthesized by Epoch Life Science).

Mosquito Rearing and Mos1-Mediated Transformation. *Ae. aegypti* mosquitoes (Liverpool strain) were maintained at 28 °C and 60 to 70% humidity, with a 14/10-h day/night light cycle. Adult mosquitoes were maintained on

10% sucrose and blood-fed using artificial membrane feeders and defibrinated sheep's blood (Colorado Serum Company). Donor plasmid was coinjected at 0.5 μg/μL with the Mos1 helper plasmid, pGL3-PUbMos1 at 0.3 μg/μL into 1-h-old embryos (37). Surviving G_0 females were mated to Liverpool males in pools of 20 to 25. G_0 males were mated individually to 5 Liverpool females and then merged into pools of 15 to 20 males. G_1 larvae were screened for GFP fluorescence using a Leica M165 FC fluorescence microscope. Positive G_1 individuals were outcrossed to Liverpool females to ensure that all transgene cassettes were stably inherited to the G_2 generation. Images were taken of pupae and mature adults (7 to 10 d postemergence) at 10× (adults, pupae) or 40× (heads, genitalia, dissected tissues) magnification using the LAS v4.5 software suite and the following settings: Gain 1, Gamma 1, greyscale (white light), or pseudocolor (509 nm).

Inverse PCR for Transgene Insertion Site Determination. Inverse PCR was used to determine the insertion site of the transgenic cassette for the N1 (generation 10) and N2 (generation 7) transgenic mosquito lines. Genomic DNA was isolated from three male adult individuals for each line, using the Quick-DNA Miniprep Kit (Zymo Research) according to the manufacturer's protocol, and with an elution volume of 50 μL H_2O. Three restrictions enzymes (Thermo Fisher), HpaI, MspI, and Bsp143I, were used to digest genomic DNA from each individual of each transgenic line. Approximately 1 μg DNA was digested for 8 h using 4 μL enzyme in a 60-μL reaction volume. Digested DNA was purified using the illustra GFX PCR DNA and Gel Band Purification Kit (GE Helathcare) with an elution volume of 50 μL H_2O. Approximately 500 ng DNA was ligated in a 400-μL reaction volume with 1 μL T4 DNA Ligase (3 Weiss Units; Promega) overnight at 16 °C. DNA was purified using the illustra GFX PCR DNA and Gel Band Purification Kit (GE Healthcare) with an elution volume of 30 μL H_2O. PCR was performed using 1 μL of the purified DNA in a 50-μL reaction volume with Q5 DNA Polymerase (New England Biolabs), in a T100 Thermal Cycler (Bio-Rad), with primers (*SI Appendix*, Table S4) specific for the Mos1 transposable element right hand arm, which is located at the 5′ terminus of the transgenic cassette (see Fig. 1*A* for transgenic constructs). One specific PCR product was observed for each of the three enzymes used, for both lines. Sequencing results for all PCR products were the same for all individuals within each line, consistent with a single insertion site for each of the transgenic lines.

Chromosome FISH. Slides of mitotic chromosomes were prepared from imaginal discs of fourth instar larvae from the N1 transgenic line following published protocols (38). FISH was performed using the N1 plasmid construct (Fig. 1*A*) as a probe and 18S rDNA as a landmark for the q arm of chromosome 1. The N1 plasmid probe was labeled by nick translation (Invitrogen), with Cy3-deoxyuridine 3-triphosphate (dUTP; Enzo Life Sciences). 18S rDNA was labeled by PCR (Bioline) with Cy5-dUTP (Enzo Life Sciences). Chromosomes were counterstained with Oxasole yellow (YOYO-1) iodide and mounted in Prolong Gold Antifade (Invitrogen). Slides were analyzed using a Zeiss LSM 510 Laser Scanning Microscope (Carl Zeiss Microimaging) at 1,000× magnification.

Endogenous and Transgenic *Nix* Transcription Profile. Transgenic *Nix* GFP+ males from line N2 (M/m; N2/+) were crossed with Liverpool strain females and blood fed. To collect aged embryos ∼20 to 30 females were placed into 50-mL conical tubes with a wet cotton ball and a disk of filter paper at the bottom. Females were allowed to lay over the interval time and then removed from the tubes and eggs allowed to mature to the desired age. Embryos were transferred from the filter paper to a 1.5-mL tube with a fine paint brush and snap-frozen in liquid nitrogen at the appropriate time. Embryos ($n \geq 100$) were collected for the following time points: 0 to 1 h, 2 to 4 h, 4 to 8 h, 8 to 12 h, 12 to 24 h, and 24 to 36 h. More eggs were collected from the same cage and hatched in order to collect siblings at all four larval stages ($n = 50$). One- and 2-d-old pupae, as well as 2- to 4-d postemergence adults were snap-frozen individually in 1.5-mL tubes so they could be genotyped by PCR before further processing (*SI Appendix*, Fig. S3). RNA was isolated using Quick-RNA Miniprep (Zymo Research). cDNA was then synthesized using the SuperScript RT kit (Life Technologies). RT-PCR was performed using Phire II DNA polymerase (Thermo Fisher Scientific) and primers are listed in *SI Appendix*, Table S4. We took advantage of the Strep-tag II inserted between the 5′UTR and the ORF of the *Nix* in the N2 construct to design primers that only amplify cDNA from the endogenous *Nix* transcript (*SI Appendix*, Table S4). Similarly, primers were also designed to only amplify the N2 transgenic *Nix* transcript (*SI Appendix*, Table S4).

Wing-Length Measurement and Statistical Analysis. Wing-length values were measured for 30 individuals from line N2, eclosed from the same cohort of

G_{14} larvae. Right wings were detached from 1-d postemergence adults, and mounted on a slide. A photograph was taken of each wing using a Leica DFC3000 G camera mounted on a Leica M165 FC Fluorescent Stereo Microscope. A 2-mm scale bar was photographed to standardize size measurements. ImageJ was used to measure the wing length as the distance from the anal lobe to the wing tip (17, 39) (*SI Appendix*, Fig. S5). Wing length values for each phenotype are reported in box plots (Fig. 2*D*) and shown in *SI Appendix*, Table S5. One-way ANOVA was performed using all samples, resulting in a *P* value of <0.0001. The Tukey simultaneous test for difference of means was performed resulting in adjusted *P* < 0.0001 for all pairwise comparisons except for transgenic males vs. wild-type males (*P* = 0.1982). A test for equal variances was performed using both Levene's method and the multiple comparisons method.

RNA-Seq. Two- to 4-d-postemergence adult siblings from the N1 transgenic line were snap-frozen in liquid nitrogen and preserved at −80 °C until the time of extraction. RNA was extracted using the Quick-RNA Miniprep kit (Zymo Research). Triplicate RNA-seq libraries were prepared for each of the four genotypes (Fig. 2*E*) using the NEBNext Ultra RNA Library Prep Kit for Illumina with the NEBNext Poly(A) mRNA Magnetic Isolation Module (New England Biolabs) and multiplexed into one lane of a HiSEq. 2500.

RNA-Seq Data Analysis. RNA-seq reads from the wild-type and transgenic mosquito samples were aligned using Tophat2 (v2.1.1) to the *Ae. aegypti* L5 reference genome. The resulting BAM files were sorted and indexed. MarkDuplicates from the Picard tool kit v1.119 was used to identify and remove PCR duplicates (broadinstitute.github.io/picard/). Cufflinks v2.2.1 was used to assemble transcripts and estimate the relative abundances of the transcripts (40). Transcription levels were estimated as fragments per kilobase per million mapped reads (FPKM). The reference transcript file (AaegL5.0.gtf) was downloaded from VectorBase (vectorbase.org). Cuffdiff, a component of Cufflinks was used to normalize and compare the transcript expression levels between samples (41). The log_2(FPKM+1) expression-level heatmaps (Fig. 2*E*) were generated using the heatmap.2 function in R's gplots package (https://www.rdocumentation.org/packages/gplots/). Both columns (samples) and rows (genes) were clustered using the default hierarchical clustering settings. Row scaling was applied and the row z-score values were used for the color scale.

ddPCR for *Doublesex* and *Fruitless* Isoforms and Data Analysis. Total RNA was isolated from each of the four genotypes using the ZymoResearch Quick-RNA MiniPrep Kit according to the manufacturer's protocol. Three adult individuals (biological replicates) were used for each sample and all were siblings from generation 9 of the N1 transgenic line. cDNA was synthesized in a 20-μL reaction volume with ∼500 ng total RNA and random hexamers, using the Invitrogen SuperScript III First-Strand Synthesis Super Mix according to the manufacturer's protocol, and the 20-μL completed cDNA reaction was diluted to a total of 60 μL with H_2O. cDNA quality was checked by PCR using primers specific for ribosomal protein S7 (Rps7). These primers span a 110-nt intron, which should yield a 501- or 611-bp PCR product for cDNA or a genomic DNA template, respectively. Primers were ordered from Sigma Aldrich. *Ae. aegypti* (Liverpool) male genomic DNA and H_2O was used as templates for positive and negative controls, respectively. PCR was performed using Phire HS II DNA polymerase from Thermo Fisher Scientific according to the manufacturer's protocol. One microliter of the cDNA reaction was used in a total of 20-μL PCR volume and run for 30 cycles on a Bio-Rad MyCycler thermal cycler. Products were size-separated on a 1% agarose gel by electrophoresis, using a 100-bp step ladder from Promega. ddPCR was performed using 1 μL of the cDNA reaction with the Bio-Rad QX100 ddPCR machine according the manufacturers protocols. Taqman assays were designed to detect sex-specific *doublesex* and *fruitless* isoforms (*SI Appendix*, Table S4). The gene AAEL002401 was used as an internal reference for gene expression (9, 42). Probes were ordered from Biosearch Technologies and primers were ordered from Sigma Aldrich. Expression values are reported as the mean $\pm$ the SEM (*SI Appendix*, Fig. S6). One-way ANOVA was performed using all samples for each assay and the Tukey simultaneous test for difference of means was performed for all pairwise comparisons (*SI Appendix*, Fig. S6). A test for equal variances was performed using both Levene's method and the multiple-comparisons method.

Mating Conditions for Flightless Males. Five-day-old virgin Liverpool females were bloodfed and immediately placed in the refrigerator for 20 to 30 min so that they became immobile. Five of these cold-anesthetized females were placed in a 50-mL plastic conical tube together with five-to-eight flightless m/m males. The cotton ball covering the tube was pushed down close to the bottom to

confine the mosquitoes to a small space to induce mating. The flightless males only had a few minutes to mate before the females became active. Mosquitoes were transferred to a 16-oz soup cup after half an hour. An egg cup was added to the soup cup after 2 d to collect eggs and embryos were hatched 5 d later.

CRISPR/Cas9-Mediated *Myo-Sex* Knockout. Genomic regions of the *myo-sex* gene were manually searched for the presence of NGG (PAM), where N is any nucleotide. Selected target sites were 5′-GAAGCCGAAGGATACGTT CA<u>AGG</u>-3′, 5′-GTAACCGTTGCTTTACCAGG<u>TGG</u>-3′, and 5′-GGTTACCAAGTC ACCCTT<u>GGTGG</u>-3′, with PAM sites underlined. sgRNAs were generated as previously described (43) using primers listed in *SI Appendix*, Table S4, in vitro-transcribed using MEGAscript T7 kit, and purified using the MEGAclear kit (Thermo Fisher Scientific). RNAs were aliquoted and stored at −80 °C. Cas9 mRNA was in vitro-transcribed, as previously described (44), and used for the first two knockout experiments (Fig. 3*B*). For the third replicate, Cas9 (ARCA) mRNA (Trilink Biotechnologies) was used. Three rounds of injections were performed with Cas9 mRNA at 0.6 μg/μL and all three sgRNAs at 0.1 μg/μL each for ~500 embryos per replicate experiment. G$_0$ males displayed a noticeable phenotype and were grouped by ability to fly, then crossed with Liverpool females. Mutations in the flightless male G$_1$ were verified using the Phire II Animal Tissue Direct PCR kit (Thermo-Fisher Scientific), following the dilution procedure utilizing a single leg for the DNA template. Primers used for mutation screening are listed in *SI Appendix*, Table S4. PCR amplicons were purified using the NucleoSpin Gel and PCR Clean-up kit (Macherey-Nagel) and sequenced.

Male Competitiveness Assay. To mitigate the effect of genetic background and rearing condition, transgenic and their nontransgenic siblings were sexed, screened, and collected at the pupal stage from the same cohort and allowed to emerge separately. Six replicate cages were set up and assayed for each line as described below. Within 48 h after emergence, 20 flying transgenic males and 20 of their nontransgenic male siblings were placed in a 44-oz cage to commingle for 3 d before 10 5-d-old wild-type Liverpool virgin females were added and allowed to mate for another 2 d before blood feeding. Females were inspected individually to ensure that they were fully engorged. Two days later each female was transferred into an egg-laying tube, which is a 50-mL plastic conical tube with a hardened 50-mm wet paper disk on top of a water-soaked cotton ball at the bottom. Three to four days after egg laying, the eggs from individual females were hatched. The hatched larvae were fed with one crushed pellet of fish food and reared in sanitary, but nutrient-rich water at an optimal density, changing water or adding food as needed. Larvae were screened at L3–L4 using the GFP fluorescence marker and the numbers of GFP$^+$ (transgenic) and GFP$^-$ (nontransgenic) were recorded.

Statistical Analysis of the Proportion of Transgenic Progeny. Statistical analyses were performed using generalized linear mixed-effects models with transgenic and nontransgenic progeny counts as the independent variables (R package *lme4*). These variables were treated as fixed-effects and individual broods nested within cages/replicates were treated as random-effects. We employed a binomial regression in the analysis to model independent variables represented as proportions. The data in each test was assessed for overdispersion using the Pearson χ^2 statistic and all assumptions of the tests were met. Statistical power of the generalized linear mixed-model tests was estimated using the *simr* package in R, with a number of iterative simulations set at 1,000. We used R v3.6.2 (45) to perform these analyses.

1. D. Bachtrog *et al.*; Tree of Sex Consortium, Sex determination: Why so many ways of doing it? *PLoS Biol.* **12**, e1001899 (2014).
2. H. Salz, J. W. Erickson, Sex determination in Drosophila: The view from the top. *Fly (Austin)* **4**, 60–70 (2010).
3. M. Hasselmann *et al.*, Evidence for the evolutionary nascence of a novel sex determination pathway in honeybees. *Nature* **454**, 519–522 (2008).
4. T. Kiuchi *et al.*, A single female-specific piRNA is the primary determiner of sex in the silkworm. *Nature* **509**, 633–636 (2014).
5. R. H. Baker, R. K. Sakai, Triploids and male determination in the mosquito, Anopheles culicifacies. *J. Hered.* **70**, 345–346 (1979).
6. U. Willhoeft, G. Franz, Identification of the sex-determining region of the Ceratitis capitata Y chromosome by deletion mapping. *Genetics* **144**, 737–745 (1996).
7. J. N. Shukla, S. R. Palli, Production of all female progeny: Evidence for the presence of the male sex determination factor on the Y chromosome. *J. Exp. Biol.* **217**, 1653–1655 (2014).
8. D. Charlesworth, J. E. Mank, The birds and the bees and the flowers and the trees: Lessons from genetic mapping of sex determination in plants and animals. *Genetics* **186**, 9–31 (2010).
9. A. B. Hall *et al.*, SEX DETERMINATION. A male-determining factor in the mosquito Aedes aegypti. *Science* **348**, 1268–1270 (2015).
10. A. B. Hall *et al.*, Radical remodeling of the Y chromosome in a recent radiation of malaria mosquitoes. *Proc. Natl. Acad. Sci. U.S.A.* **113**, E2114–E2123 (2016).
11. E. Krzywinska, N. J. Dennison, G. J. Lycett, J. Krzywinski, A maleness gene in the malaria mosquito Anopheles gambiae. *Science* **353**, 67–69 (2016).
12. F. Criscione, Y. Qi, Z. Tu, GUY1 confers complete female lethality and is a strong candidate for a male-determining factor in *Anopheles stephensi*. *eLife* **5**, e19281 (2016).
13. A. Sharma *et al.*, Male sex in houseflies is determined by *Mdmd*, a paralog of the generic splice factor gene *CWC22*. *Science* **356**, 642–645 (2017).
14. A. Meccariello *et al.*, *Maleness-on-the-Y* (*MoY*) orchestrates male sex determination in major agricultural fruit fly pests. *Science* **365**, 1457–1460 (2019).
15. B. J. Matthews *et al.*, Improved reference genome of Aedes aegypti informs arbovirus vector control. *Nature* **563**, 501–507 (2018).
16. T. G. M. Schmidt, A. Skerra, The Strep-tag system for one-step purification and high-affinity detection or capturing of proteins. *Nat. Protoc.* **2**, 1528–1535 (2007).
17. R. M. Gleiser, J. Urrutia, D. E. Gorla, Body size variation of the floodwater mosquito Aedes albifasciatus in Central Argentina. *Med. Vet. Entomol.* **14**, 38–43 (2000).
18. L. J. Cator, B. J. Arthur, A. Ponlawat, L. C. Harrington, Behavioral observations and sound recordings of free-flight mating swarms of Ae. Aegypti (Diptera: Culicidae) in Thailand. *J. Med. Entomol.* **48**, 941–946 (2011).
19. A. B. Hall *et al.*, Insights into the preservation of the homomorphic sex-determining chromosome of Aedes aegypti from the discovery of a male-biased gene tightly linked to the M-locus. *Genome Biol. Evol.* **6**, 179–191 (2014).
20. S. O'Leary, Z. N. Adelman, Disrupting female flight in the vector Aedes aegypti. *bioRxiv*: 10.1101/862300 (2 December 2019).
21. X. Jiang, J. K. Biedler, Y. Qi, A. B. Hall, Z. Tu, Complete dosage compensation in Anopheles stephensi and the evolution of sex-biased genes in mosquitoes. *Genome Biol. Evol.* **7**, 1914–1924 (2015).
22. M. E. Helinski *et al.*, Evidence of polyandry for Aedes aegypti in semifield enclosures. *Am. J. Trop. Med. Hyg.* **86**, 635–641 (2012).
23. O. Dudchenko *et al.*, De novo assembly of the *Aedes aegypti* genome using Hi-C yields chromosome-length scaffolds. *Science* **356**, 92–95 (2017).
24. P. Juneja *et al.*, Assembly of the genome of the disease vector Aedes aegypti onto a genetic linkage map allows mapping of genes affecting disease transmission. *PLoS Negl. Trop. Dis.* **8**, e2652 (2014).
25. P. Schliekelman, S. Ellner, F. Gould, Pest control by genetic manipulation of sex ratio. *J. Econ. Entomol.* **98**, 18–34 (2005).
26. G. Fu *et al.*, Female-specific flightless phenotype for mosquito control. *Proc. Natl. Acad. Sci. U.S.A.* **107**, 4550–4554 (2010).
27. Z. N. Adelman, Z. Tu, Control of mosquito-borne infectious diseases: Sex and gene drive. *Trends Parasitol.* **32**, 219–229 (2016).
28. P. A. Papathanos *et al.*, A perspective on the need and current status of efficient sex separation methods for mosquito genetic control. *Parasit. Vectors* **11** (suppl. 2), 654 (2018).
29. V. M. Gantz *et al.*, Highly efficient Cas9-mediated gene drive for population modification of the malaria vector mosquito Anopheles stephensi. *Proc. Natl. Acad. Sci. U.S.A.* **112**, E6736–E6743 (2015).
30. C. Noble, J. Olejarz, K. M. Esvelt, G. M. Church, M. A. Nowak, Evolutionary dynamics of CRISPR gene drives. *Sci. Adv.* **3**, e1601964 (2017).
31. J. Champer *et al.*, A toxin-antidote CRISPR gene drive system for regional population modification. *Nat. Commun.* **11**, 1082 (2020).
32. J. Champer *et al.*, Resistance is futile: A CRISPR homing gene drive targeting a haplolethal gene. bioRxiv:10.1101/651737 (27 May 2019).
33. A. Simoni *et al.*, A male-biased sex-distorter gene drive for the human malaria vector Anopheles gambiae. *Nat. Biotechnol.*, 10.1038/s41587-020-0508-1 (2020).
34. A. Beaghton, P. J. Beaghton, A. Burt, Gene drive through a landscape: Reaction-diffusion models of population suppression and elimination by a sex ratio distorter. *Theor. Popul. Biol.* **108**, 51–69 (2016).

35. A. Burt, Site-specific selfish genes as tools for the control and genetic engineering of natural populations. *Proc. Biol. Sci.* **270**, 921–928 (2003).
36. M. A. Anderson, T. L. Gross, K. M. Myles, Z. N. Adelman, Validation of novel promoter sequences derived from two endogenous ubiquitin genes in transgenic Aedes aegypti. *Insect Mol. Biol.* **19**, 441–449 (2010).
37. C. J. Coates, N. Jasinskiene, L. Miyashiro, A. A. James, Mariner transposition and transformation of the yellow fever mosquito, Aedes aegypti. *Proc. Natl. Acad. Sci. U.S.A.* **95**, 3748–3751 (1998).
38. V. A. Timoshevskiy, A. Sharma, I. V. Sharakhov, M. V. Sharakhova, Fluorescent in situ hybridization on mitotic chromosomes of mosquitoes. *J. Vis. Exp.*, e4215 (2012).
39. E. Van Handel, J. F. Day, Correlation between wing length and protein content of mosquitoes. *J. Am. Mosq. Control Assoc.* **5**, 180–182 (1989).
40. A. Roberts, C. Trapnell, J. Donaghey, J. L. Rinn, L. Pachter, Improving RNA-Seq expression estimates by correcting for fragment bias. *Genome Biol.* **12**, R22 (2011).
41. C. Trapnell *et al.*, Differential analysis of gene regulation at transcript resolution with RNA-seq. *Nat. Biotechnol.* **31**, 46–53 (2013).
42. W. Hu, Z. J. Tu, Functional analysis of the promoter of an early zygotic gene KLC2 in Aedes aegypti. *Parasit. Vectors* **11** (suppl. 2), 655 (2018).
43. A. R. Bassett, C. Tibbit, C. P. Ponting, J. L. Liu, Highly efficient targeted mutagenesis of Drosophila with the CRISPR/Cas9 system. *Cell Rep.* **4**, 220–228 (2013).
44. S. Basu *et al.*, Silencing of end-joining repair for efficient site-specific gene insertion after TALEN/CRISPR mutagenesis in Aedes aegypti. *Proc. Natl. Acad. Sci. U.S.A.* **112**, 4038–4043 (2015).
45. R version 3.6.2. https://www.r-project.org. Accessed 8 July 2020.

AGRICULTURAL SCIENCES